HIGH THERMAL CONDUCTIVITY, MESOPHASE PITCH-DERIVED CARBON FOAM

James Klett

Carbon and Insulation Materials Technology Group, Metals and Ceramics Division,
Oak Ridge National Laboratory, Oak Ridge, TN, 37831-6087

ABSTRACT

A relatively simple technique for fabricating mesophase pitch-based carbon foam has been developed at Oak Ridge National Laboratory. This technique produces graphitic foam with an open cell structure and an extremely high bulk thermal conductivity, >100 W/m·K. The cell walls have a highly aligned graphitic structure, similar to high-performance carbon fibers, exhibiting interlayer spacing (d_{002}) of 0.336 nm, coherence length ($L_{a,100}$) of 203 nm, and a stacking height ($L_{c,002}$) of 442 nm. Consequently, the foam cell walls (struts) exhibit a thermal conductivity between 700 and 1,200 W/m·K. Because of the low density (ρ) of 0.5 g/cm^3, the specific thermal conductivity of the foam is more than four times greater than that of copper.

KEY WORDS: Carbon Foam, High Thermal Conductivity, and Mesophase Pitch

1. INTRODUCTION

The extraordinary mechanical properties of carbon fiber result from the unique graphitic morphology of the spun (extruded) filaments (1). Contemporary advanced structural composites exploit these properties by creating a disconnected network of graphitic filaments held together by a matrix suitable for the application. Carbon foam derived from a pitch precursor, on the other hand, can be considered as an interconnected network of graphitic ligaments and, thus, should exhibit isotropic material properties (2, 3). The foam represents a potential reinforcing phase for structural composite materials. Because of the continuous graphitic network, the foam-reinforced composites will display higher isotropic thermal conductivities than carbon fiber reinforced composites. Furthermore, the lack of interlaminar regions, which develop in traditional prepregged carbon fiber reinforced composites, should result in enhanced mechanical properties such as shear strength and fracture toughness.

Recent research into fiber-reinforced composites has been driven by the need for increased mechanical properties such as strength, stiffness, creep resistance, and toughness in structural engineered materials. Such improvements have been achieved through the enhancement of fiber properties, fiber/matrix interfaces, and matrix materials.
In recent years the use of carbon fibers has evolved from structural reinforcement to a thermal management material, with the emphasis in applications such as high-density electronic modules, communication satellites, and automotive systems. The high cost of carbon fibers has stimulated research into both novel reinforcements and new composite processing methods. Other than low cost, the primary concerns in thermal management applications are high thermal conductivity, low weight, and low coefficient of thermal expansion (4). Such applications have focused on sandwich structures (a high thermal conductivity material encapsulating a structural core material) to provide the required

mechanical properties (4). However, since structural cores are typically low-density materials, the thermal conductivity of the overall composite through the thickness is relatively low (~3-10 W/m·K for aluminum honeycomb (5, 6)). Metallic foams are being explored as a potential core material; however the thermal conductivities are still low, 5 - 50 W/m·K (6). New pitch-derived graphitic foams present a unique solution to this problem by offering high thermal conductivity with a low weight.

In order to produce high stiffness and high conductivity graphitic foams a mesophase pitch must be used as the precursor, thus assuring a graphitic structure in the struts (2, 7, 8). Typical processes utilize a blowing technique, or pressure release, to produce foam of the pitch precursor (7, 9-12). The pitch foam is stabilized by heating in air or oxygen for many hours to cross-link the structure and "set" the pitch so it does not melt during further heat treatment (13). Stabilization is a very time consuming process and can be expensive (depending on the part size and equipment required). The "stabilized" pitch is carbonized in an inert atmosphere to temperatures as high as 1100°C, and graphitized at temperatures as high as 3000°C to produce a thermally conductive graphitic structure.

A new, less time consuming process for fabricating pitch-based graphitic foams without the traditional blowing and stabilization steps has been developed. It is believed that this new foam will be less expensive and easier to fabricate than traditional foams. Therefore, it should lead to a significant reduction in the cost of carbon-based thermal management and structural materials (i.e. foam reinforced plastics and foam core composites).

2. EXPERIMENTAL

2.1 Foam Processing. The foam is produced via a proprietary method developed at Oak Ridge National Laboratory in the Carbon and Insulation Materials Technology Group. The process does not utilize a thermodynamic flash (blowing) agent to produce the foam and, most importantly, the unique method eliminates the requirement to stabilize the foamed pitch prior to carbonization (typically an oxidative stabilization step). The method is fairly versatile and can be easily adjusted to control pore/cell size and density. For this research, three mesophase pitches were used to produce graphitic foam: Mitsubishi ARA24 naphthalene-based synthetic pitch, and two propriatary mesophase pitches from Conoco Corporation labeled Conoco A and Conoco B. The properties of each pitch are listed in Table 1. All foam samples were graphitized at 5°C/min in Argon to 2800°C and soaked for 1 hour.

Samples of the graphitized ARA pitch-derived foam were vacuum impregnated with an epoxy resin [100 parts DER (Dow) 332 resin mixed with 46 parts of Jeffamine T-403 (Huntsman) hardener] to produce a foam-reinforced composite with a density of 1.26 g/cm^3. Some samples of the graphitized ARA pitch-derived foam were densified with carbon by vapor phase (methane) deposition to a final density of 1.3 g/cm^3.

Table 1. Properties of mesophase pitch used to produce graphitic foam.

Mesophase	Softening Point [°C]	Mesophase Content [%]	Carbon Yield @1000 °C, N_2
Mitsubishi ARA24	237	100	78
Conoco A	285	100	73
Conoco B	355	100	87

2.2 Foam Characterization. The physical characteristics of the foams, such as surface area and pore diameter, were measured on a Micromeritics Autopore II 9220 mercury porosimeter. In order to develop a fundamental understanding of the foam structure and graphitic morphology, several examination techniques were employed. Optical microscopy with cross-polarized light and a first-order red wavelength retarder were performed on a Nikon Microphot-FXA microscope. Samples were examined using a JOEL scanning electron microscope. X-ray diffraction data were taken with a Scintag PAD V powder diffractometer, using Cu Kα radiation.

Compression testing was performed to characterize the strength and stiffness of the foam and foam-reinforced composites (not all samples were fully characterized due to lack of material). Compression tests were performed on ½-in diameter x ½-in thick samples using ASTM standard C695-91 on an Instron test rig with a 1000 lb. load cell.

The thermal conductivity of the foam was measured with two different techniques. First, a xenon flash diffusivity technique was performed on samples ½-in. diameter by ½-in. thick on a custom built machine in the High Temperature Materials Laboratory at Oak Ridge National Laboratory. Also, thermal conductivity was measured on ½-in. x ½-in. by 1-mm thick samples with a thermal interface tester using the thermal gradient method at a major computer chip manufacturer.

3. RESULTS AND DISCUSSION

3.1 Processing All three mesophase pitches produced acceptable foams, although the two with low melting points produced foams with a density gradient. The Mitsubishi ARA 24 and the Conoco-A pitches produced foams with the lower 50% of the foam exhibiting a density of about 0.55 g/cm^3 and the upper 50% exhibiting a density of about 0.35 g/cm^3. Figure 1 is typical foam produced from Mitsubishi ARA 24 pitch prior to carbonization. The lower density material was weaker than the dense material. This became evident as the samples were physically handled. The low-density portion would crumble, while the dense portion could be handled without damage. Henceforth, only the dense portion of these foams will be discussed.

The Conoco B pitch produced foam with no density gradient. It is believed that this is because of the higher melting point of the pitch and a narrower temperature bandwidth at which decomposition gases evolve. A more viscous fluid combined with a shorter foaming period prevents settling and coalescing of the bubbles, virtually eliminating the gradient.

Figure 1.   Foam produced from ARA24 mesophase pitch.

3.2 Characterization Table 2 presents the physical characteristics of the foams after graphitization. The foams produced from the two pitches with low melting points had similar densities, but significantly different mean pore diameters and specific surface areas. On the other hand, the foam produced from the high melting point mesophase pitch (Conoco B) had both a lower density and mean pore diameter with a significantly higher specific surface area. Figure 2 is a SEM micrograph of the Mitsubishi foam illustrating that the foam exhibits a predominately open cell structure.   The struts of the foam appear completely different from vitreous glassy carbon foams produced commercially; the struts being significantly thicker and exhibiting a spherical structure. The layering effect visible in the struts shows that the material is graphitic

Figures 3 (a) and (b) are optical micrographs under cross-polarized light. It is clear that from the micrograph of the struts (Figure 3(a)), that the graphene layer planes are highly oriented parallel to the surface of the bubbles. As the foam is produced, the shear stresses from the expansion of the bubbles cause the liquid mesophase crystals to align parallel to the surface of the bubbles. During carbonization and graphitization, the resultant aligned carbon forms the highly ordered graphitic structures. The lack of an oxidative stabilization allows the crystals to form very large graphitic crystals. Figure 3(b) is a high magnification picture of the junctions of the struts, illustrating that the region is highly graphitic, but there is more fold-sharpening and crystal misalignment in these regions. These regions will serve to weaken the foam structurally and reduce the overall thermal conductivity.

Table 2. Properties of graphitic foams produced from different precursors.

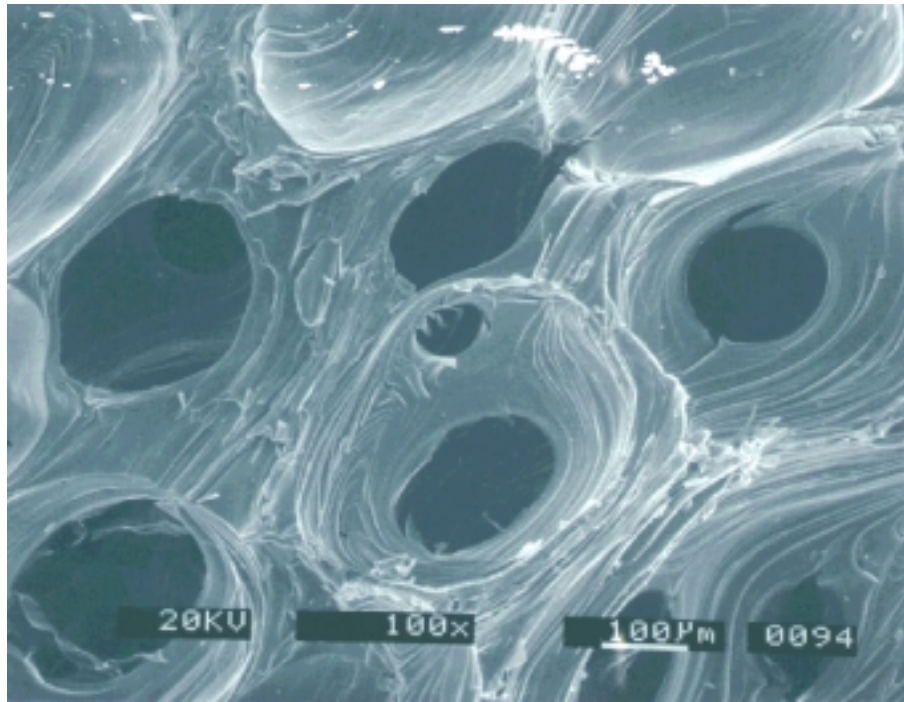| Foam	Density [g/cm^3]	Mean Pore Diameter [μm]	Specific Surface Area m^2/g
Mitsubishi ARA24	0.54	93	4.0
Conoco A	0.52	114	2.0
Conoco B	0.46	73	7.2

Figure 2.   Scanning electron micrograph of ARA pitch-derived foam graphitized at 2800°C.
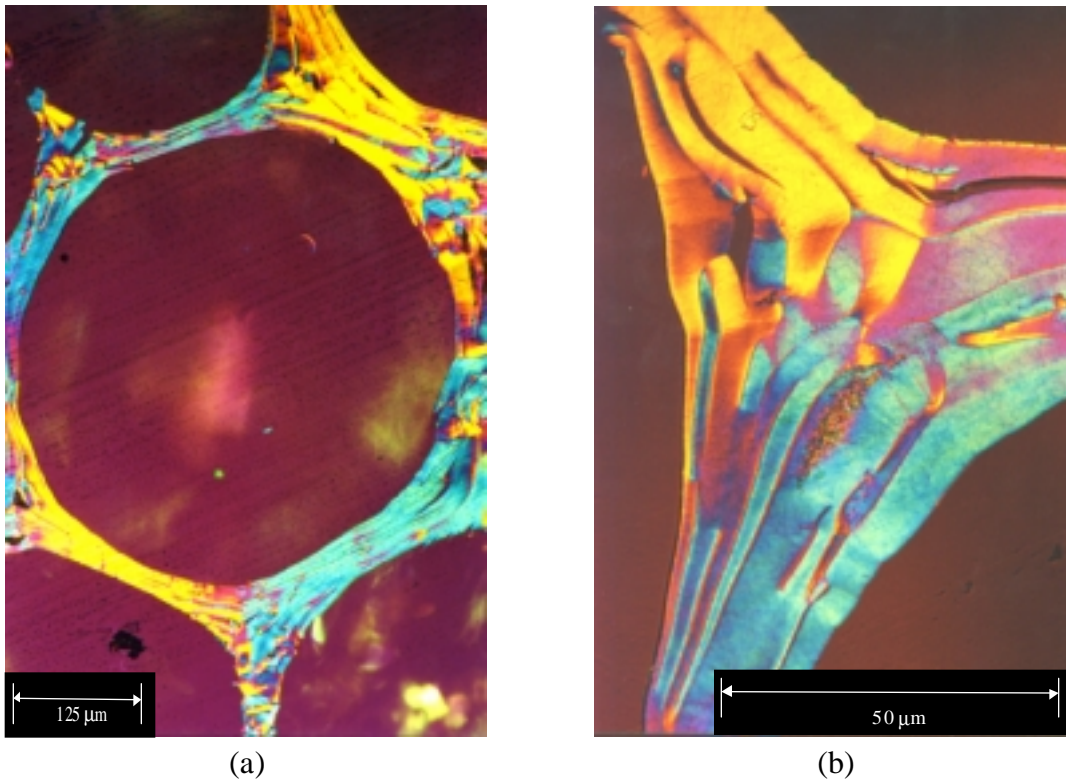

125 µm

(a)

50 µm

(b)

Figure 3.   Optical micrograph of ARA pitch-derived foam graphitized at 2800°C illustrating the struts (a) at 40x and the junctions between the struts (b) at 100X.

3.3 X-ray Analysis Lattice parameters were determined from the indexed diffraction peak positions. The X-ray method for crystallite size determination has been extensively reviewed elsewhere (14). The 002 and 100 diffraction peak breadths were analyzed using the Scherrer equation to determine the crystallite dimensions in the a- and c- directions.

$$t = \frac{0.9\lambda}{B\cos(2\theta)},$$

where t is the crystallite size, λ is the X-ray wavelength, B is the breadth of the diffraction peak (full width half maximum (FWHM) minus the instrumental breadth), and 2θ is the diffraction angle.

As shown in Figure 4, the 002 peak (which is characteristic of interlayer spacing), was very narrow and asymmetric, indicative of highly ordered graphite.   The interlayer spacing calculated with the Scherrer method was 0.3362 nm, significantly closer to pure graphite (0.3354 nm) than most high performance pitch derived carbon fibers (15). Table 3 is a comparison of heat treatment temperatures and X-Ray diffraction results of the graphite foam and various carbon fibers (15). The foam has the lowest d-spacing and the highest degree of graphitization.   The crystallite size in the c-direction was calculated from these data to be 442 nm, and the 100 peak (or $10\bar{1}0$ in hexagonal nomenclature) was used to calculate the crystallite size in the a-direction of 203 nm. These crystallite sizes are larger than typical high thermal conductivity carbon fibers (15, 16), and therefore, the foam material should perform similarly to high order pyrolytic carbon and high thermal conductivity carbon fibers such as K1100 and vapor grown carbon fibers (VGCF).
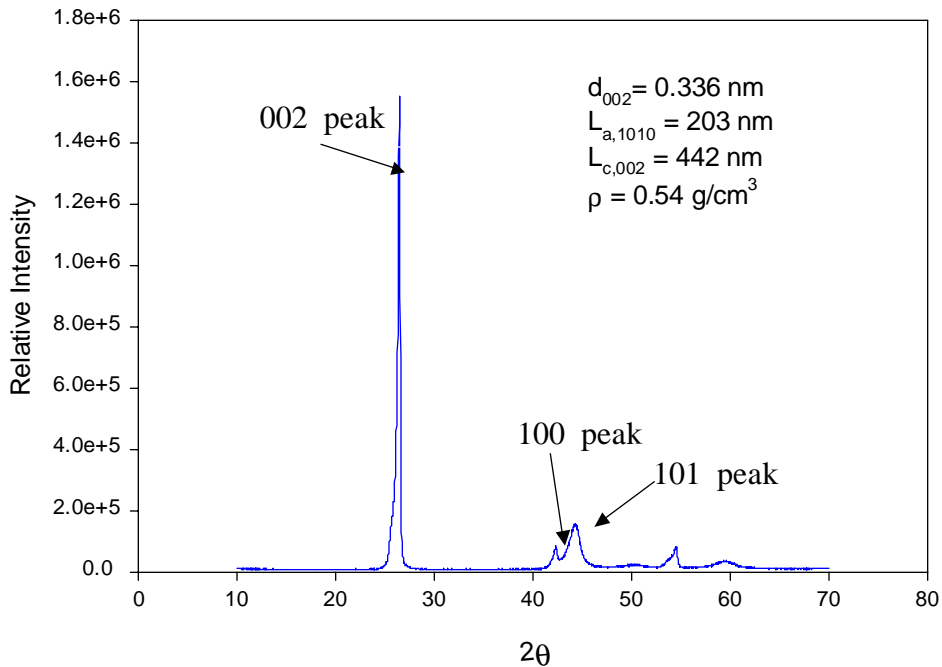

Figure 4.   X-ray analysis of graphtized foam (2800°C).

Table 3. Comparison of X-Ray diffraction results and the degree of graphitization of various carbon fibers and the graphite foam.

Material	Heat Treatment	d-spacing	g_p*
	[°C]	[nm]	[%]
PAN fiber [15]	2500	.342	23
P-120 (pitch) [15]	--	.3392	56
Floating catalyst VGCF [15]	--	.3385	64
Fixed catalyst VGCF [15]	--	.3449	--
Fixed catalyst VGCF [15]	2200	.342	23
Fixed catalyst VGCF [15]	2800	.3366	86
Graphitized Foam	**2800**	**.3362**	**91**

*g_p= degree of graphitization and is defined as (0.3440-d-spacing)/(0.3440-0.3354) where 0.3440 and 0.3354 are the d-spacing of turbostratic graphite and single crystal (perfect) graphite (15).

3.4 Mechanical Properties The mechanical properties of the foam and foam-based composites are presented in Table 4. The compressive strength of the foam was rather low (3.4 MPa) compared to carbon fibers. However, it compares well with aluminum and Kevlar® honeycombs. When the samples were impregnated with the epoxy resin the compressive strength increased by an order of magnitude to 34.3 MPa, and the flexural strength, 19.5 MPa, approached that of commercial thermal management panels. Although similar compressive strengths, 31.6 MPa, and flexural strengths, 19.4 MPa, were achieved when the foam was densified with CVD carbon, the mode of failure was different, as shown in Figure 4. While both the raw graphitic foam and the resin filled foam exhibited a high work of fracture, the CVD/foam material had a more brittle failure.

Table 4. Mechanical properties of foam and other thermal management panels.

| Material	Specific Gravity	Flexural		Compressive	
		Strength	Modulus	Strength	Modulus
		MPa	**GPa**	**MPa**	**GPa**
ARA Foam	*0.54*			*3.4*	*.180*
ARA Foam /Epoxy	*1.26*	*19.5*	*--*	*34.3*	*.560*
ARA Foam /Carbon CVI	*1.3*	*19.4*	*2.3*	*31.6*	*.850*
EWC – 300X [17] K1100 (4K PW)/ERL 1939-3 resin	1.72	29.5†	13.1†	18.5	--
Aluminum Honeycomb [5] (CRIII 5052) ⅛ -in. cell size, 1 mil wall	0.07	--	--	3.7	1.030
Aluminum Honeycomb [5] (CRIII 5052) ⅛ -in. cell size, 3 mil wall	0.19	--	--	18.6	1.030
Kevlar Honeycomb [5] (HRH®-49) ¼" cell size	0.03	--	--	0.90	.172
Aluminum Foam [18]	0.5	--	--	~1.0	~1.0

†Tensile properties.
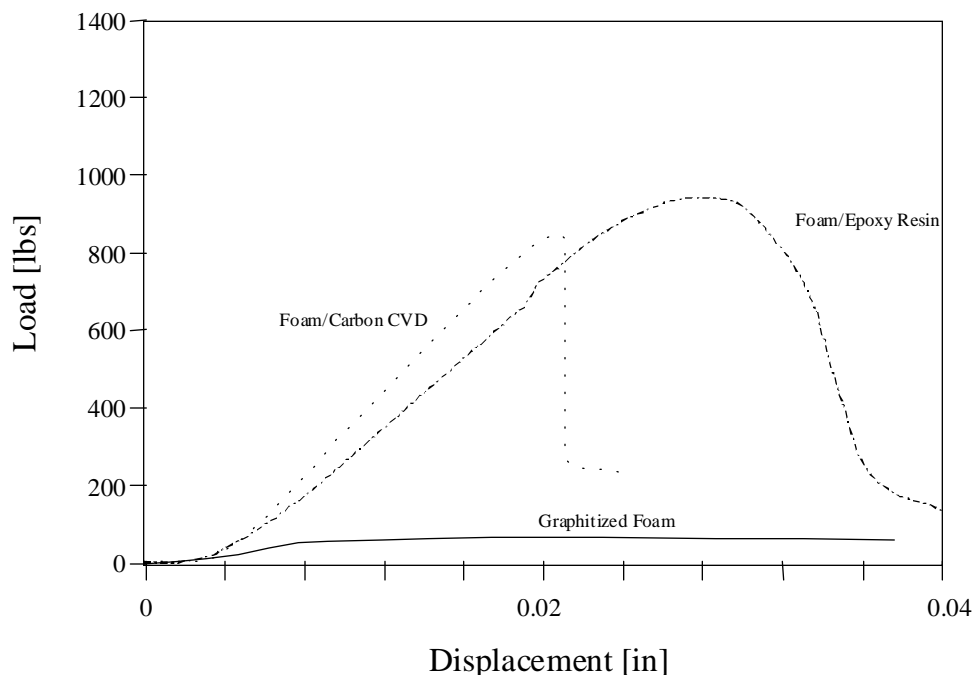
Figure 4.   Compression tests of ARA 24 Pitch-derived carbon foam and foam derived composites.

3.5 Thermal Diffusivity The validity of the flash diffusivity method and whether the open porosity would permit penetration of the heat pulse into the sample had to be established. Deep penetration of the pulse in samples typically causes a change in the characteristic heat pulse on the back face of the sample. Thus, errors in the reported diffusivity can be as high as 20% (19). However, the rather large struts and small openings of the foam limits the depth of penetration to about two pore diameters (140-220 µm), or less than 2% penetration. Therefore, it was believed that this technique would yield a fairly accurate value for the thermal conductivity. This was confirmed by testing samples with both the flash diffusivity method (20) and the thermal gradient method (21). The measured conductivities varied by less than 5%, verifying the flash method as a viable method to measure these foams. If the pore structure changes significantly, the flash method will likely yield inaccurate results.

The thermal diffusivity of the foam was very high as shown in Table 5.   The thermal conductivity of the graphitized ARA 24 foam was as high as 106 W/m·K. This is remarkable for a material with such a low density, 0.54 g/cm^3. The foam exhibits thermal conductivies comparable to the in-plane thermal conductivity of some other thermal management materials and significantly higher than in the out-of-plane directions of the other thermal management materials. Although several of the other thermal management materials have higher in-plane thermal conductivities, their densities are much greater than the foam, i.e., the specific thermal conductivity of the foam is significantly greater than all the available thermal management panels. In fact, the specific thermal conductivity is more than four times greater than copper, the preferred material for heat sinks.

It is clear that for thermal management, where weight is a concern or where un-steady state conditions occur often, the graphitic foam is superior to most other available materials. The advantage of isotropic thermal and mechanical properties should allow for novel designs that are more flexible and more efficient.

Table 5. Thermal properties compared to composite thermal management panels

	Specific Gravity	Thermal Conductivity		Specific Thermal Conductivity*	
		In-plane	Out-of-plane	In-plane	Out-of-plane
		[W/m·K]	[W/m·K]	[W/m·K]	[W/m·K]
ARA Foam	*0.54*	*106*	*106*	*198*	*198*
Other Thermal Management Materials					
EWC – 300X K1100 (4K PW)/Cyanate Matrix [17]	1.72	29.5	13.1	17	7
Copper [17]	8.9	400	400	45	45
Copper(10%)-Tungsten [17]	6.5	180	180	27	27
Copper(70%)- EWC-300X (K1100) [17]	6.5	240	100	36	15
K321 (3K phenolic densified) [22]	1.6	54.8	8.3	34	5
K321 (2K AR pitch densified) [22]	1.88	233.5	20.4	123	11
Aluminum Honeycomb [5] (CRIII 5052) $\frac{1}{8}$ -in. cell size, 1 mil wall	0.07	--	~5	--	71
Aluminum Honeycomb [5] (CRIII 5052) $\frac{1}{8}$ -in. cell size, 3 mil wall	0.19	--	~10	--	142
Aluminum Foam [18]	~0.5	12	12	24	24

*defined as thermal conductivity divided by specific gravity

3.6 Applications

3.6.1 Internal Combustion Engines A piston for internal combustion engines made from a foam-reinforced aluminum (rather than the more conventional aluminum alloy) will have higher creep resistance and lighter weight, thus improving efficiency and reducing emissions. Also, foam-reinforced plastics could be utilized as a piston or engine block material. Although some plastics can withstand the temperature of an internal combustion engine (not generally higher than 300°C), the low thermal conductivity of the plastic prevents heat removal during the cycles. Therefore, the system overheats and the plastic melts or decomposes. However, a carbon foam-reinforced plastic will have a thermal conductivity similar to aluminum pistons (which typically don't experience temperatures higher than 300°C), and therefore should remove heat at a similar rate to aluminum pistons. A cyanate ester/foam piston will save as much as 40% the weight of the pistons, reducing the slung weight of the engine. This will increase power output and improve efficiency. It is even conceivable that the entire engine block could be made from a foam-reinforced polymer.

3.6.2 Heat Exchangers The combination of open porosity and large specific surface achieved with the foam allows for the improvement of heat exchangers. If the shell side of the exchanger is filled with the high thermal conductivity foam, there will be effectively several orders of magnitude increase in surface area to transfer heat to the working fluid (preferably a gas due to the pressure drop). Heat will be rapidly transferred from (or to) the shell side fluid through the foam, and then to the heat exchanger tubing and the tube side fluid. Such an increase in surface area will allow for a reduction in size of the heat exchanger, offsetting the increase in pressure drop through the foam. A reduction in size of heat

exchanger will reduce weight and improve efficiency in many applications, such as automobiles and aircraft.

4. CONCLUSIONS

The manufacture and properties of a high thermal conductivity foam have been reported here. The existence of very sharp 002 and 100 peaks confirms that the graphite crystals are very large and are highly graphitic (nearly 91%). Under cross-polarized light, very large monochromatic regions in the struts of the foam are visible, suggesting that these struts will behave like high thermal conductivity carbon fibers, such as K1100 and VGCF. In fact, the d-spacing and crystallite sizes were better than VGCF, which have a thermal conductivity as high as 1950 W/m·K. These properties, combined with the continuous graphite network throughout the foam, result in an isotropic thermal conductivity greater than 100 W/m·K and a specific conductivity over 4 times that of copper, an industry standard for thermal management. While the mechanical properties were similar to honeycomb structures, the isotropic thermal conductivity of a foam-core composite will provide far superior thermal management characteristics. This should lead to more efficient thermal management materials.

The densified foam test data indicate that the foam can be utilized as a replacement for carbon fiber in some applications, thereby reducing costs. This should allow carbon reinforced plastics, carbon, ceramics, and metals to enter markets not usually considered.

Although the data and discussion presented in this paper illustrate the potential of this material to be an enabling technology for many applications, significantly more work is needed. The ability to add chopped fibers and particulates to control pore size, thermal conductivity, and mechanical properties must be evaluated. A full characterization of the kinetics of the foaming reaction must be undertaken in order to allow optimization of the process. The effects of different pitches on the foam characteristics need to be studied. The ability to produce a gradient in the material might be of interest in some applications. Finally, the effects of pore size on the mechanical and thermal properties should be evaluated.

5. REFERENCES

1. D. D. Edie, Carbon Fibers, Filaments, and Composites, Edited by J. L. Figueiredo, et. al., Kluwer Academic Publishers, pp. 43-72 (1990).
2. W. Hagar and Max L. Lake, Mat. Res. Soc. Symp., 270, 29-34 (1992).
3. Hagar, W. and Max L. Lake, Mat. Res. Soc. Symp., 270, 41-46 (1992).
4. Shih, Wei, "Development of Carbon-Carbon Composites for Electronic Thermal Management Applications," IDA Workshop, May 3–5, 1994, supported by AF Wright Laboratory under Contract Number F33615-93-C-2363 and AR Phillips Laboratory under Contract Number F29601-93-C-0165.
5. Hexcel Product Data Sheet (1997).
6. Gibson, L. J., Mat. Sci. and Eng., A110, 1-36 (1989).
7. Hagar, W. and Max L. Lake, Mat. Res. Soc. Symp., 270, 35-40 (1992).
8. White, J. L., and P.M. Sheaffer, Carbon, 27 (5), 697-707 (1989).
9. Gibson, L.J., and M. F. Ashby, Cellular Solids: Structures & Properties, Pergamon Press, New York (1988).
10. Knippenberg, W. F., and B. Lersmacher, Phillips Tech. Rev., 36 (4), 93-103 (1976).
11. Aubert, J. H., Mat. Res. Soc. Symp., 207, 117-127 (1990).

12. Cowlard, F. C., and J. C. Lewis, J. of Mat. Sci., 2, 507-512 (1967).
13. Kearns, Kris, "Graphitic Carbon Foam Processing," 21st Annual Conference on Ceramic, Metal, and Carbon Composites, Materials, and Structures, Janyary 26-31, Cocoa Beach, Florida, pp. 835-847 (1997).
14. H.P. Klug and L.E. Alexander X-Ray Diffraction Procedures for Polycrystalline and Amorphous Materials, 2nd edn., J. Wiley, New York, USA, (1974).
15. Lake, M., *Mat. Tech.*, 11 (4), 131-144 (1996).
16. Jones, S. P., C.C. Fain, and D. D. Edie, Carbon, 35 (10), 1533-1543 (1997).
17. Amoco Product Literature (1997).
18. Steiner, K., J. Banhard, J. Baumister, and M. Weber, "Production and Properties of Ultra-Lightweight Aluminum Foams for Industrial Applications," Proceeding from the 4th International Conference on Composites Engineering, Edited by David Hui, July 6-12, pp. 943-944 (1997).
19. Inoue, K., High Temp. Tech., 8 (1), 21-26 (1990).
20. Cowan, R. D., J. of App. Phys., 34 (4), 926-927 (1962).
21. Kobayashi, K., J. Japan Welding Soc., 561, 38-42 (1987).
22. Olhlorst, C. W., W. L. Vaughn, P. O. Ransone, and H-T Tsou, "Thermal Conductivity Database of Various Structural Carbon-Carbon Composite Materials," NASA Technical Memorandum 4787, November 1997.

ACKNOWLEDGEMENTS